FMGM 2015 – PM Dight (ed.)

Quarrying-induced subsidence investigated by combining contact and remote monitoring systems

F Bozzano *Sapienza University of Rome, Italy*

C Esposito *Sapienza University of Rome, Italy*

P Mazzanti *NHAZCA S.r.l., Sapienza University of Rome, Italy*

A Rocca *NHAZCA S.r.l., Sapienza University of Rome, Italy*

Abstract

This work focuses on a multidisciplinary study carried out in an urban area located 20 km east of Rome, Italy affected by subsidence (and related structural damages) induced by dewatering related to quarrying activities.

An intense monitoring activity has been carried out in order to understand the spatial and temporal evolution of the process by using both contact and remote sensing methodologies.

Underground geological setting has been derived thanks to geotechnical investigations carried out by means of more than 90 boreholes. The hydrogeological variations occurred in the last decades as the response to the anthropic stress, has been obtained by a 3D numerical model based on a large piezometric monitoring dataset.

Single buildings have been monitored by means of levelling and total stations, while on site instruments to monitor the groundwater levels (electric cluster piezometers) and in depth ground deformation (assestimeter) have been installed.

On larger scale, multi-temporal aerial photos have been analysed to infer the increase of quarrying exploitation, whereas satellite A-DInSAR analyses have been carried out at different scales in order to achieve information about past displacements.

This comprehensive set of data allowed us to describe the space and time distribution of the subsidence process.

1 Introduction

The Acque Albule basin is a quite flat area located about 20 km east of Rome which is affected by a relevant subsidence process clearly testified by significant damages to several buildings related to differential settlements (Figure 1). In terms of structural damages, the subsidence process started to involve buildings in the mid-1980s and increased at the beginning of the 2000s, even causing the evacuation of some houses and public buildings. In the first instance, it is possible to state that several potential predisposing/ triggering factors for the observed subsidence are present in the study area: (i) the presence of compressible soils in the upper few metres of the local substratum; (ii) a continuously growing urbanisation (with related overloads); (iii) a very significant groundwater exploitation (and related water table lowering) due to the presence of a variety of 'anthropic stresses', i.e. quarry activities and several agricultural and domestic wells. With particular regard to the quarrying activities, it should be noted as such activities have expanded significantly in recent decades, thus involving new portions of territory previously not-disturbed (Figure 2).

The study presented here aims at defining the recent time history of ground deformations by means of advanced DInSAR techniques (A-DInSAR), to be compared with the piezometric variations (both measured and simulated by means of numerical modelling) and the stratigraphic setting (obtained by interpolating

data from several available and purpose drilled boreholes), in order to better understand and constrain the relationships among subsidence (in terms of both magnitude and rate), timing of piezometric level variations and thickness of compressible soils. It is worth noting that the methodologies and results presented here at the basin scale are framed within a research project (PRIN 2010) funded by Italian Ministry of Education, University and Research (MIUR): within this project an experimental test site has been equipped with multi-base electric piezometers and an assestimeter for a very detailed analysis of the cause-effect relationships among subsidence rate, pore water pressure variations and stratigraphical/geotechnical setting of subsoil.

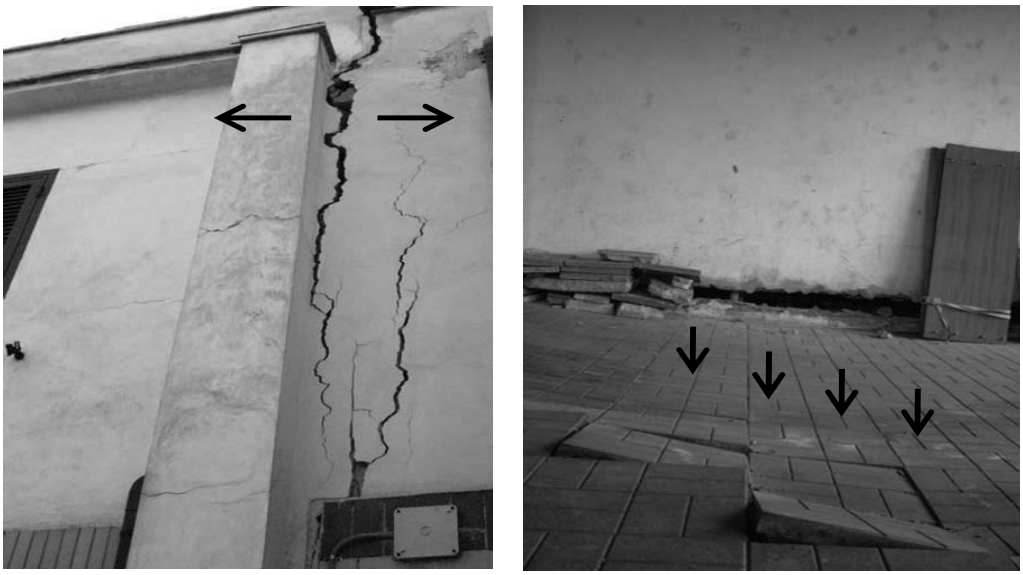

(a) (b)

Figure 1 Effects on buildings induced by the subsidence in the study area; examples of structural (a) and non-structural (b) damages

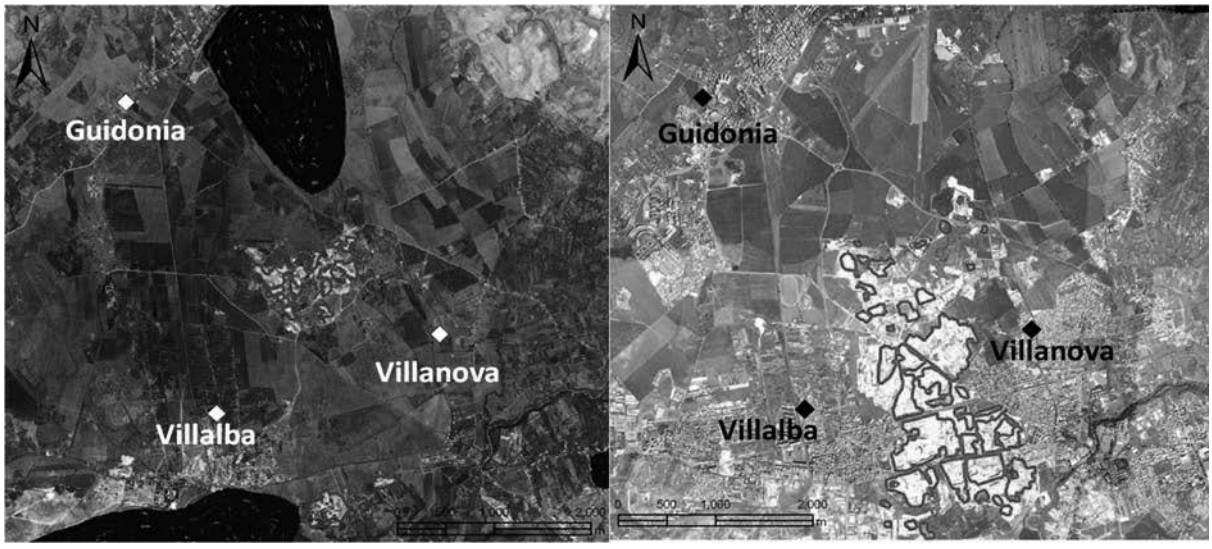

(a) (b)

Figure 2 Evolution of the quarries activities in the plain: (a) the orthophoto represents the plain in 1954: the perimeter of each pit is shown by polygons; some obscured areas are depicted such as the Guidonia airport to the north, as required by the military regulations at the time; (b) the orthophoto represents the plain in 2005: the perimeter of each pit is shown by polygons. It is clear the huge expansion of the quarries area (modified from Floris et al. 2014)

2 A-DInSAR methodology

In recent years, Synthetic Aperture Radar Interferometry (InSAR) technology has proved its capability in deriving high accuracy (up to few millimetres) ground and structure deformation information from Synthetic Aperture Radar (SAR) images (Curlander & McDonough 1991). Comparing with other traditional methods, InSAR technology is favoured for its capability to provide monitoring data all-time, with all-weather conditions and especially for wide-areas. The other relevant key-factor of InSAR-based monitoring is the possibility to perform past-oriented deformation measurements thanks to archive SAR data made available by National and International Space Agencies.

The first satellite missions with SAR sensors were launched in the early 1990s and since then images have been collected in several parts of the world and revisited over same area several times each year. For example, the minimum time interval between images collected by the Envisat-ASAR sensor is 35 days even if some temporal gaps, due to problems in the satellite acquisition, can be present.

In addition, thanks to the development of new X-Band high-resolution SAR satellites, namely TerraSAR-X (TSX) launched by German Space Agency (DLR) and COSMO-SkyMed (CSK) by the Italian Space Agency (ASI), the potential for monitoring man-made structures with high accuracy is more achievable. The new sensors provide one order of magnitude higher spatial resolution than previously available satellite SAR sensors, in addition to their shorter revisit time (11 days for TSX and up to four days for CSK).

The basic elements to perform InSAR analyses are the SAR images acquired by satellites. SAR images consist of a matrix made of resolution cells (i.e. pixels) whose size depends on the satellite sensor (usually ranges between few metres up to few tenths of metre) that contains information about the satellite-target distances.

In order to overcome the major limits of InSAR technique, whose most important is the presence of the atmospheric phase screen (APS) disturbance, the Advanced Differential InSAR (A-DInSAR) methods were proposed to successfully perform ground and structure deformation measurement thanks to long time series of SAR images (Ferretti et al. 2001; Berardino et al. 2002). By analysing several SAR images acquired in the same area over time, A-DInSAR methodology allows derivation of displacement-time information of natural targets on the ground that are visible from the satellite (Figure 3).

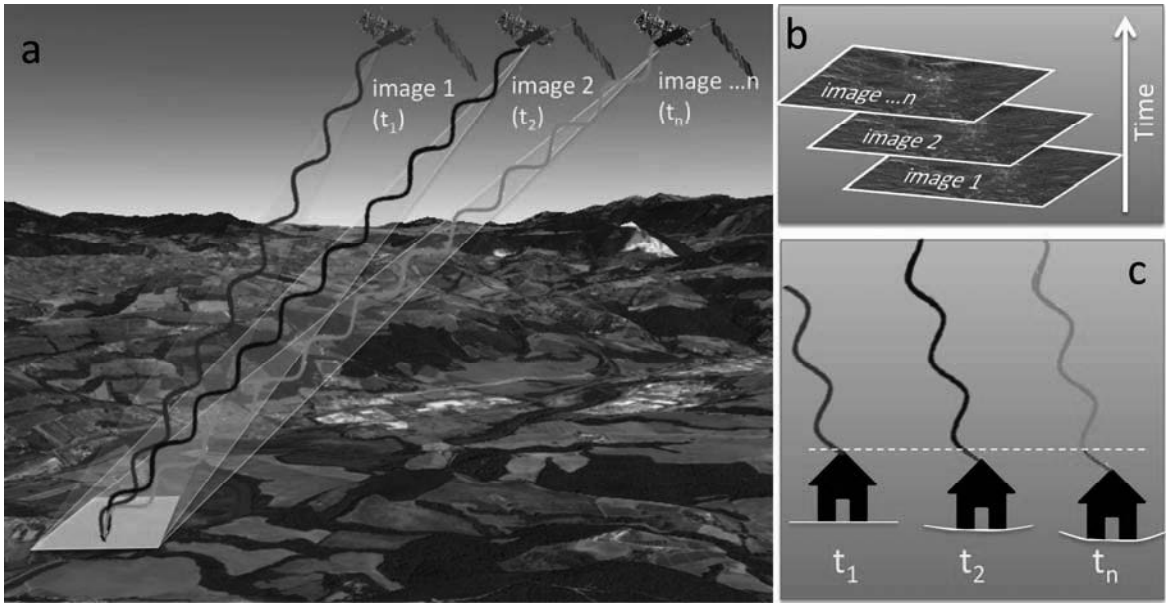

Figure 3 Sketch of A-DInSAR principles: (a) multi-pass satellite acquisitions; (b) image stacking; (c) phase difference of the multi-temporal SAR signal used to infer displacement related to good radar targets

Since only displacements along the satellite line of sight (LOS) can be measured, combinations of data acquired from different points of view allow improvement of displacement orientation information. In fact

SAR images can be acquired in two different orbital geometries: during the passage of the satellite from North to South (descending geometry), and from south to north (ascending geometry). Hence, the same area can be observed by two angles of view almost symmetrical.

Among the characteristics of A-DInSAR, one of the most effective is based on the analysis of measurement points characterised by a high and stable radar reflectivity over time. This is the basic principle of the A-DInSAR method known as 'persistent scatterers interferometry' (PSI) (Ferretti et al. 2001). Usually such good targets are buildings, roads, railways, pylons and structures such as dams, bridges as well as exposed rocks and portions of homogeneous soil. Once the measurement points have been detected, the electromagnetic phase signals reflected by targets on the surface of the earth can be used to infer several data. These include (i) the trend of deformation during the whole time period covered by the images; (ii) the time series of displacement, starting from the first available data, with an accuracy up to some millimetres; (iii) the height of the target w.r.t. the ground; (iv) cyclic (non-linear) deformation due to several factors (e.g. temperature variations).

3 Geological and hydrogeological background

The Acque Albule Basin is a morphotectonic depression, whose formation and development is related to the Plio-Quaternary activity of strike-slip tectonic elements (Figure 4). The so formed depression, whose bedrock is featured by meso-cenozoic limestone, hosted the deposition of Plio-Pleistocene alluvial, lacustrine, and epivolcanic deposits. These deposits are in turn covered by a thick (up to 80 m) travertine cover, well known since the Ancient Roman age with the name of Lapis Tiburtinus. Such a travertine cover is mainly made up of stiff and cemented calcite, whose precipitation and growth occurred in several phases between 115-30 kPa (Billi et al. 2007; Faccenna et al. 2008; 1994) and is strictly connected with the deep hydrothermal circulation into the Meso-Cenozoic limestone. Moving upward within the stratigraphic sequence, the travertine plateau is overlaid by a discontinuous cover of a weakly cemented up to loose travertine, composed by clasts interspersed in a sandy-silty matrix. Finally, the development of karst collapses within the travertine caused the formation of morphological depressions which hosted a lacustrine-palustrine environment with the deposition of sandy silts, clay-loam (with high organic content) and peats.

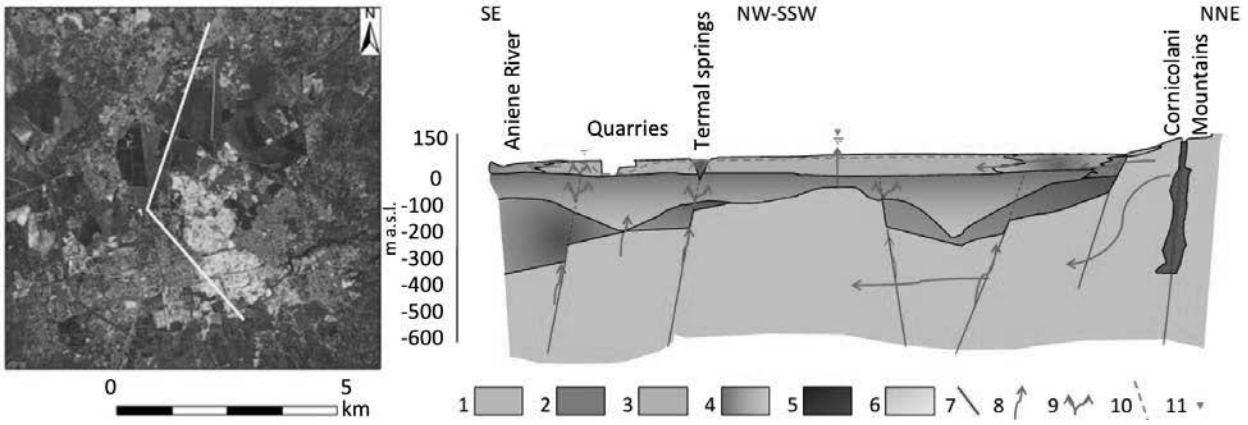

Figure 4 Simplified geological and hydrogeological cross-section of the Acque Albule Basin. Key to legend: (1) recent alluvial and colluvial deposits; (2) debris; (3) travertine and lacustrine/palustrine deposits; (4) pleistocene deposits; (5) pliocene deposits; (6) carbonatic bedrock; (7) fault; (8) flow direction; (9) groundwater overspill; (10) water table level; (11) confined water table level. Modified after Capelli et al. (2005)

The last two geological units (namely, loose travertine sandy silts and organic clay-loam and peat), that in a first instance can be grouped in a 'compressible' geological-technical unit, have a quite variable thickness below the ground level, ranging between few centimetres up to more than 10 metres, as revealed by the geological model interpolated on the basis of available stratigraphic logs (Figure 5).

Strictly related to the quite complex geological setting is the multi-level groundwater circulation in the Acque Albule Basin (Figure 4). The Meso-Cenozoic limestone hosts a deep aquifer fed laterally by the deepest part of the surrounding carbonate ridges, outcropping east and north-east of the basin. The water contained herein is thermalised due to the rise of deep fluids at high pressure and temperature from the supply system of the Colli Albani volcanic complex, which outcrops southward. The aquifer is confined at the top by clayey-sandy deposits that act as aquitard/aquiclude thus providing a piezometric level even higher than the ground level. The aquitard separates the deep aquifer from the most superficial hosted in the travertine plateau and fed by contributions directly from rainfall and laterally by the above mentioned surrounding carbonate ridges. In addition, such an aquifer is partially fed by the upwelling of thermalised waters (and gas), coming from the deep aquifer and passing through the tectonic discontinuities which drove the formation of the basin itself (Boni et al. 1986; Capelli et al. 1987; Faccenna et al. 2008; Faccenna 1994). Several springs with significant discharge testify for the huge potential of such an aquifer.

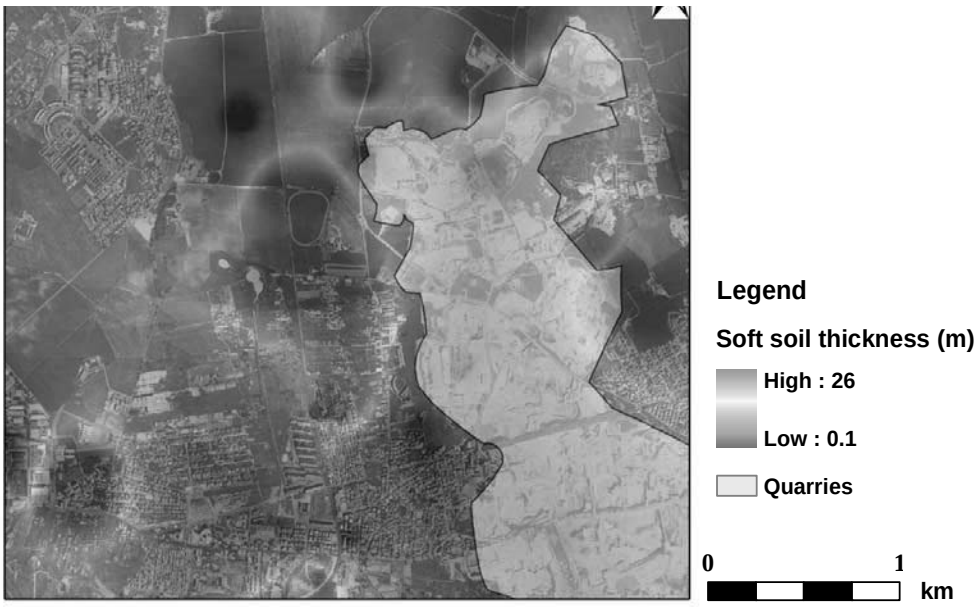

Figure 5 Map representing the spatial distribution of soft soil thickness

Notwithstanding, the 'superficial' aquifer is stressed by human activities so much that the water balance is unstable: a generalised lowering of the water table affects a wide portion of the Acque Albule Basin, while a more significant dewatering (and related piezometric level lowering) involves the areas surrounding the travertine quarries where water pumping (on the order of 4 m^3/s) is necessary to exploit deep travertine banks. Such a quarrying activity increased in the last decades (Figure 2), thus causing a progressive enlargement and deepening of the related cone of depression. Based on the collection of hydrogeological monitoring data as well as on hydrodynamic parameters, a detailed hydrogeological 3D numerical model was performed by updating and refining a previous one (Brunetti et al. 2013). Such a model allowed us to reconstruct with a good degree of confidence the 'time history' of the dewatering process over time and space (Figure 6).

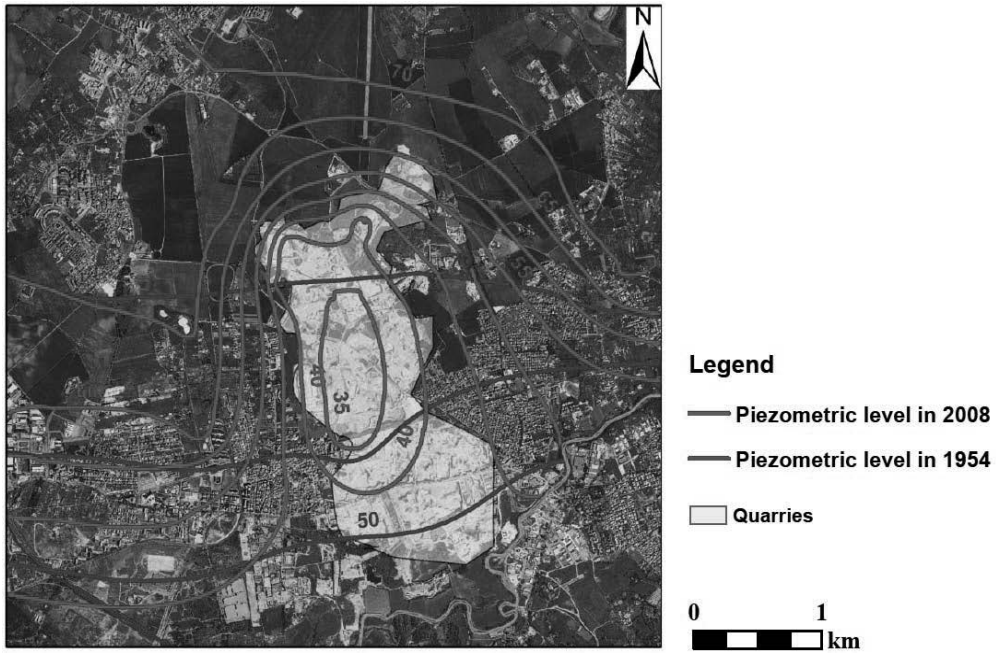

Figure 6 Reconstruction via numerical modelling of piezometric levels (m a.s.l.) within travertine in undisturbed (1954) and disturbed (2008) conditions

4 Interferometric analyses

The above depicted geological and hydrogeological framework is robust enough to more deeply understand the relative weight of different factors in the activation of subsidence, once the 'time history' of ground deformation is reconstructed by means of SAR data. In this work, ground subsidence measurements were obtained by using PSInSAR technique (Ferretti et al. 2000; 2001; Hooper et al. 2004; Kampes 2006) and using proprietary procedures implemented in SARPROZ© software (Perissin & Wang 2012; Perissin et al. 2011).

The analysis was carried out through two main approaches: full-site processing (Figure 7) and local scale processing (Figure 9). Full-site processing allowed us to reconstruct the deformational trend of the entire basin, with the aim of characterising a large portion of territory in terms of mean annual LOS velocity. Additional analyses were performed on a local scale and focused on areas of greatest interest, in order to identify possible non-linear trends correlated with piezometric level variations caused by human activity.

ERS and ENVISAT data stacks, provided by ESA in the frame of the CAT-1 project 'Geological reconstruction and monitoring in recently urbanised areas affected by subsidence' (ID: 13097), both in ascending and descending acquisition geometry, were processed independently and combined only as final geocoded products in a GIS system: use was made of 192 Synthetic Aperture Radar (SAR) scenes, covering the period June 1993-August 2010. For each path and frame we selected a single master and co-registered all slave images to that master.

With regard to full-site analyses, PS candidates (PSC) were selected based on a combination of several quality parameters related to the amplitude of the radar signal (reflectivity and ASI). A network of PSC was created to estimate preliminary height and velocity parameters, in order to retrieve and remove the APS. After APS removal, a secondary parameter estimation was performed on a wider set of points, selected on a spatial coherence and ASI combination criterion. For the displacement parameter, a linear deformation trend model was adopted. At the end of the PS analyses, all PSs with coherence above 0.65 were selected. For each PS, LOS velocity, displacement time series and height were computed (related to a reference point identified in a stable area outside the Acque Albule Basin).

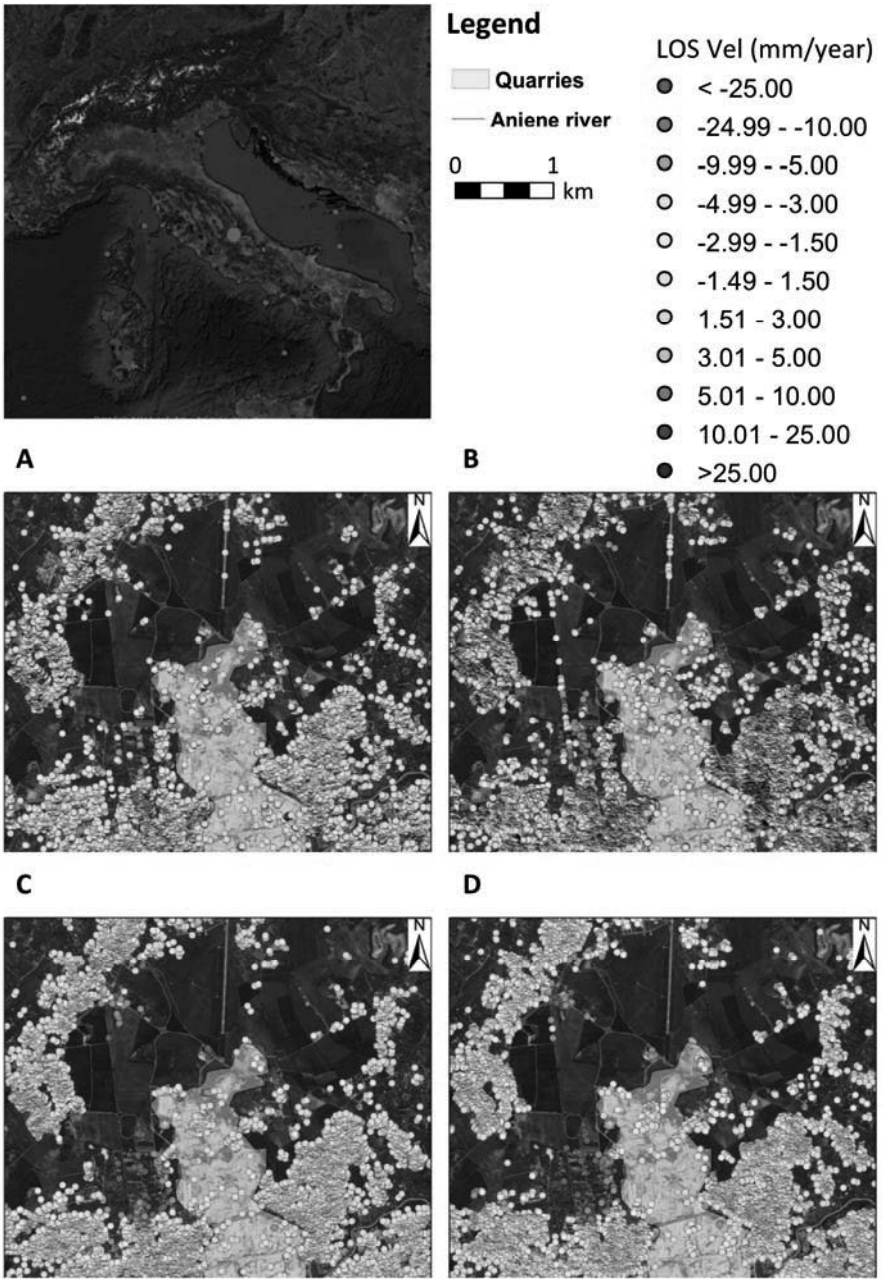

Figure 7 Maps of the mean annual subsidence rate along LOS obtained by processing satellite images from ERS ascending (A), ERS descending (B), ENVISAT ascending (C) and ENVISAT descending (D)

The analysis at local scale, carried out to highlight non-linear and/or cyclical deformation, was performed on the portion of the basin that was progressively involved in the dewatering. Several sectors (with an area smaller than 2 km^2) of the basin were analysed separately. This approach does not require the estimation and removal of APS because we can assume that atmospheric perturbations have a correlation distance smaller than 1 km (Hanssen 2001). In contrast, non-linear movements are expected to show smaller correlation in space; thus, we assumed to be able to detect such movements via a low pass filter in time domain. The choice of the reference point for each area was performed selecting it in stable areas outside of the basin. PSC were then chosen by applying a threshold value on ASI. For the selected points, height and displacement were estimated and deformation time series were reconstructed.

5 Results

In first instance, by comparing the classified post map of the full-site PS analysis (Figure 7) and the map representing the distribution of compressible soil thickness (Figure 5), it is possible to observe in general terms the relationship between subsidence average rate and geological setting.

Furthermore, if the 'time history' of some selected PS is compared to the modelled piezometric level variations over time, an acceleration of the subsidence process can be pointed out in correspondence with the main dewatering phases (Figure 8), thus confirming the relevant role of water pumping. When water is pumped from the travertine aquifer, whose piezometric level roughly coincided with the ground level in undisturbed conditions, a gradient is created thus implying a water flow from the topmost compressive soils down to the travertine aquifer. As a result, pore pressure decreases and the soil undergoes a consolidation process. At the same time, Figure 8 shows the different behaviour of the PSs as a function of the local stratigraphy, being comparable to the dewatering magnitude.

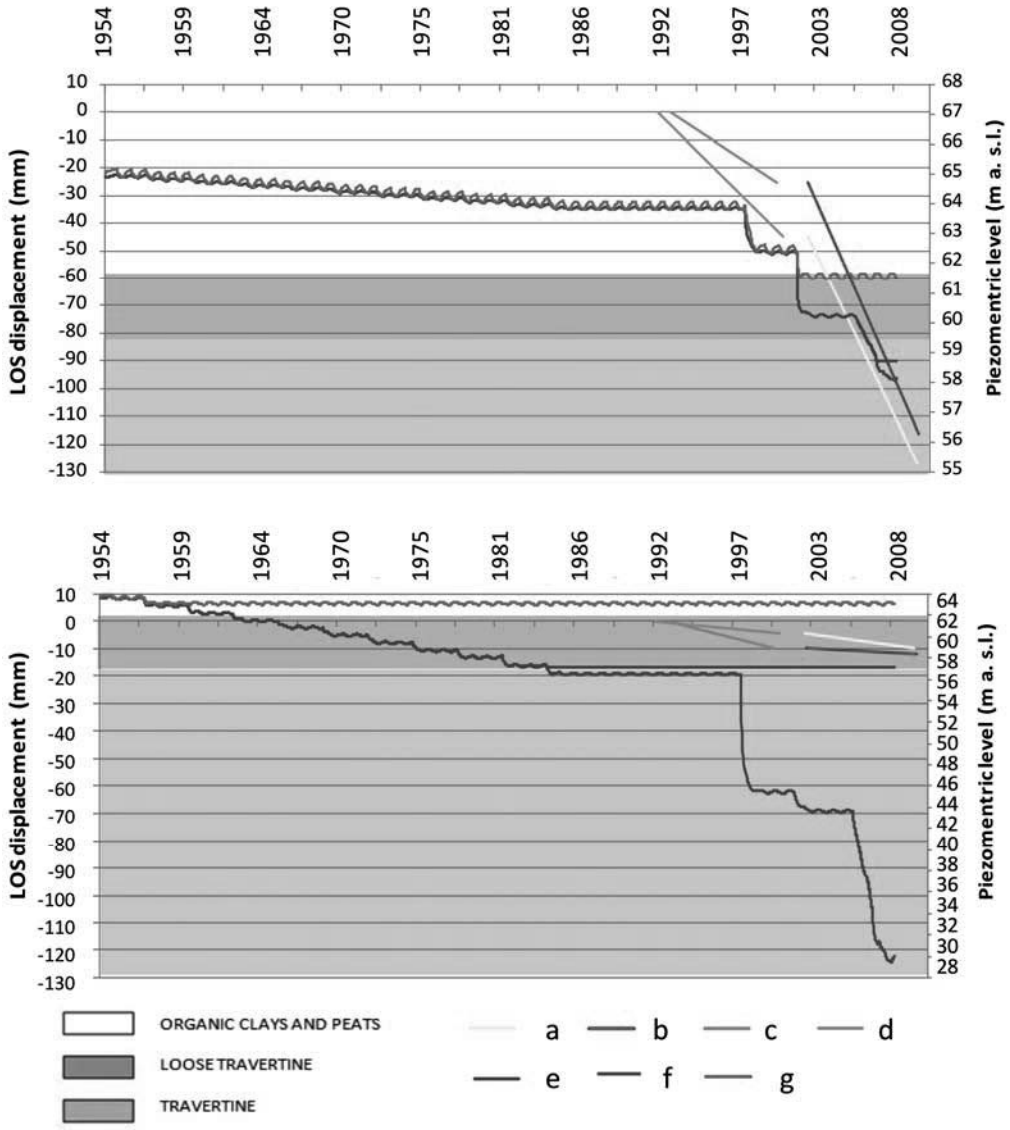

Figure 8 Charts showing the relationships between the time histories of modelled dewatering and LOS displacement in two different stratigraphic settings. Key to legend: (a) ENVISAT descending; (b) ENVISAT ascending; (c) ERS ascending; (d) ERS descending; (e) simulated piezometric level in travertine;(f) simulated piezometric level in loose travertine; (g) simulated piezometric level in organic clays and peats

More detailed hints derive from the local scale analysis: in this paper we show the results from an area located at the NW border of the basin, which is particularly significant as: (i) it encompasses a variety of stratigraphic settings; (ii) it has been involved in the cone of depression recently, so that significant piezometric variations can be noted in the investigated time interval (2001-2010).

Figure 9 clearly shows that the activation time of subsidence is strictly related to the involvement in the cone of depression, while the magnitude of the process is governed by the local stratigraphy. This evidence is testified by the behaviour of some PSs farther away from the pumping 'epicenter' that experience greater vertical movements than other points located closer: the associated stratigraphy reveals a thicker layer of compressible soils in the former points with respect to the latter ones. Finally, as expected, PSs located on the outcropping volcanic units are not affected by significant vertical deformations.

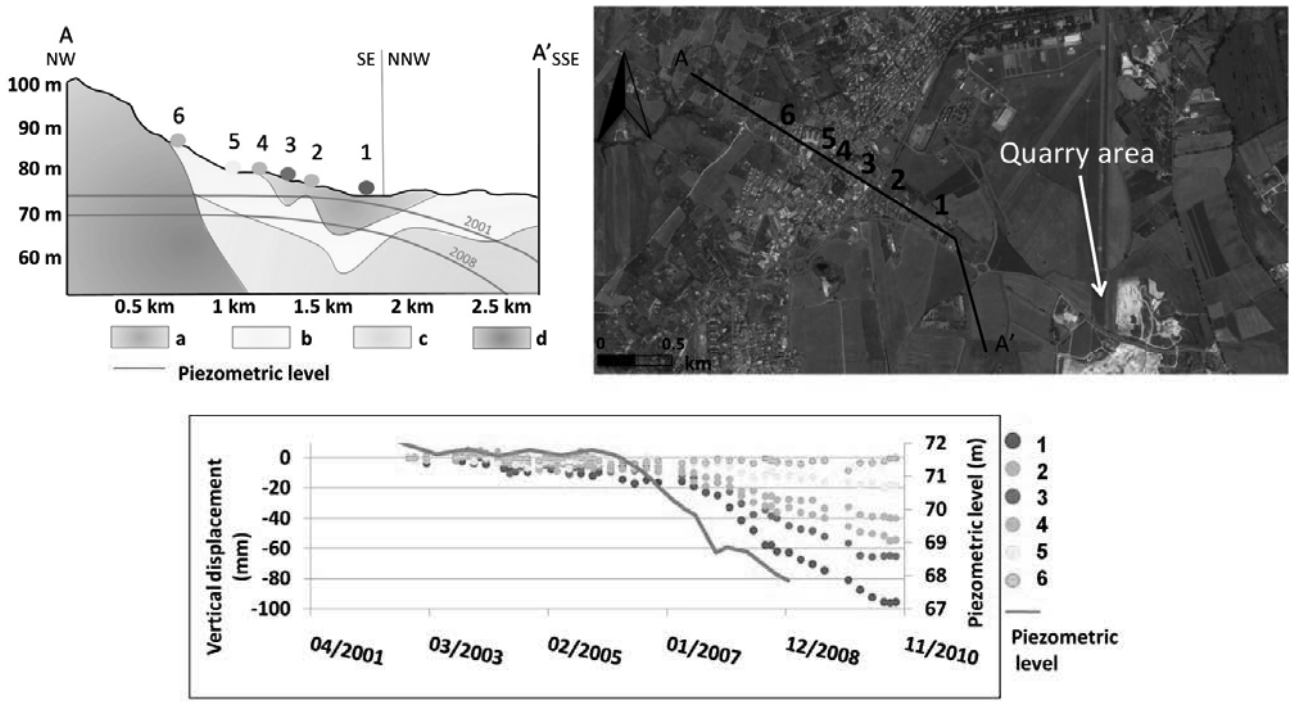

Figure 9 A-DInSAR results of a local-scale analysis performed in the northwestern sector. We reported the geological sketch (with a strong vertical exaggeration) associated with the selected PSs as well as their location. Chart showing the relationships between the time history of modelled dewatering and vertical displacement of selected PSs along the section. Key to legend: (a) organic clays and peats;(b) loose travertine; (c) travertine; (d) volcanic and sedimentary bedrock

6 Conclusion

Using the combination of geological and geotechnical data with hydrogeological modelling calibrated on piezometric data-set, we were able to explain the spatial and temporal evolution of a subsidence process related to the groundwater exploitation mainly related to quarrying activities. The subsidence process has been detected and measured in the time interval 1993-2010 by satellite A-DInSAR analyses carried out by means of four different datasets acquired in double orbital geometries (ascending and descending).

The specific role of the main controlling factors has been well constrained by the diagnosis performed here of the occurred subsidence process: the groundwater level variations drive the timing of subsidence triggering over the area, whereas the local geological conditions — namely the thickness of the compressible soils overlying the travertine hosting the exploited aquifer — drive the magnitude of the deformation process.

The results presented here encourage the research toward the forecasting subsidence processes evolution caused by groundwater exploitation in geologically well-known areas. The comprehension of factors that

control onset and development of subsidence can lead to the final aim of attempting to forecast subsidence activation and magnitude on the basis of piezometric monitoring coupled with a detailed knowledge of the geological-technical model of the subsoil. In this sense, a contribution for future outcomes could derive from the aforementioned hydrogeological/geotechnical experimental test site aimed at better quantifying the relationships among water level/pressure variations, geological setting and geotechnical properties.

References

Berardino, P, Fornaro, G, Lanari, R & Sansosti, E 2002, 'A new algorithm for surface deformation monitoring based on small baseline differential SAR interferograms', *IEEE Transactions on Geoscience and Remote Sensing*, vol. 40, no. 11, pp. 2375-2383.

Billi, A, Valle, A, Brilli, M, Faccenna, C & Funiciello, R 2007, 'Fracture-controlled fluid circulation and dissolutional weathering in sinkhole-prone carbonate rocks from central Italy', *Journal of Structural Geology*, vol. 29, no. 3, pp. 385-395.

Boni, C, Bono, P & Capelli, G 1986, 'Schema idrogeologico dell'Italia Centrale [Hydrogeological scheme of Central Italy]', *Memorie - Società Geologica Italiana*, vol. 35, pp. 991-1012.

Brunetti, E, Jones, JP & Petitta, M 2013, 'Assessing the impact of large-scale dewatering on fault-controlled aquifer systems: a case study in the Acque Albule basin (Tivoli, central Italy)', *Hydrogeology Journal*, vol. 21, pp. 401-423.

Capelli, G, Cosentino, D, Messina, P, Raffi, R & Ventura, G 1987, 'Modalità di ricarica e assetto strutturale dell'acquifero delle sorgenti Capore - S. Angelo (Monti Lucretili - Sabina Meridionale)', *Geologica Romana*, vol. 26, pp. 419-447.

Capelli, G, Mazza, R & Taviani, S 2005, 'Studi idrogeologici per la definizione degli strumenti operativi del piano stralcio per l'uso compatibile delle risorse idriche sotterranee nell'ambito dei sistemi acquiferi prospicienti i territori vulcanici laziali'. Relazione inedita, Università degli Studi di Roma III, Dipartimento di Scienze Geologiche, laboratorio di Idrogeologia (in Italian).

Curlander, JC & Mcdonough, RN 1991, *Synthetic aperture radar: systems and signal processing*, John Wiley & Sons, New York, USA.

Faccenna, C 1994, 'Structural and hydrogeological features of Pleistocene shear zones in the area of Rome (central Italy)', *Annali di Geofisica*, vol. 37, no. 1, pp. 121-133.

Faccenna, C, Funiciello, R & Mattei, M 1994, 'Late Pleistocene N-S shear zones along the Latium Tyrrhenian margin: structural characters and volcanological implications', *Bollettino di Geofisica Teorica ed Applicada*, vol. 36, pp. 507-522.

Faccenna, C, Soligo, M, Billi, A, De Filippis, L, Funiciello, R, Rossetti, C & Tuccimei, P 2008, 'Late Pleistocene cycles of travertine deposition and erosion, Tivoli, Central Italy: possible influence of climate changes and fault-related deformation', *Global Planetary Change*, vol. 63, no. 4, pp. 299-308.

Ferretti, A, Prati, C & Rocca, F 2000, 'Non-linear subsidence rate estimation using permanent scatterers in differential SAR interferometry', *IEEE Transactions on Geoscience and Remote Sensing*, vol. 38, no. 5, pp. 2202-2212.

Ferretti, A, Prati, C & Rocca, F 2001, 'Permanent scatterers in SAR interferometry' *IEEE Transactions on Geoscience and Remote Sensing*, vol. 39, no. 1, pp. 8-20.

Floris, M, Bozzano, F, Strappaveccia, C, Baiocchi, V & Prestininzi, A 2014, 'Qualitative and quantitative evaluation of the influence of anthropic pressure on subsidence in a sedimentary basin near Rome', *Environmental Earth Sciences*, vol. 72, no. 11, pp. 4223-4236.

Hanssen, RF 2001, *Radar interferometry: data interpretation and error analysis*, Springer Netherlands, Netherlands, 308 p.

Hooper, A, Zebker, H, Segall, P & Kampes, B 2004, 'A new method for measuring deformation on volcanoes and other natural terrains using InSAR Persistent Scatterers', *Geophysical Research Letters*, vol. 312, no. 23.

Kampes, BM 2006, *Radar Interferometry: Persistent Scatterer Technique*, Springer Netherlands, Netherlands, 211 p.

Perissin, D & Wang, T 2012, 'Repeat-Pass SAR Interferometry With Partially Coherent Targets', *IEEE Transactions on Geoscience and Remote Sensing*, vol. 50, no. 1, pp. 271-280.

Perissin, D, Wang, Z & Wang, T 2011, 'The SARPROZ InSAR tool for urban subsidence/manmade structure stability monitoring in China', *Proceedings of the 34th International Symposium on Remote Sensing of Environment (ISRSE 2010)*.